EFFECTS OF INTRINSIC NONLINEAR FIELDS IN THE J-PARC RCS

H. Hotchi*, F. Noda, Y. Irie, JAEA, Tokai, Ibaraki, JAPAN
S. Machida, CCLRC, RAL, ASTeC, Chilton, Didcot, Oxon, UK
A. Yu. Molodojentsev, KEK, Tsukuba, Ibaraki, JAPAN

Abstract

The 3-GeV rapid-cycling synchrotron (RCS) of J-PARC is designed to accelerate 8.3×10^{13} protons per pulse at a repetition rate of 25 Hz for the injection energy of 400 MeV. In order to realize such a high intense operation with as small particle losses as possible, a large acceptance is secured at the RCS. In such a machine with large bore, intrinsic nonlinear magnetic fields play a significant role, and the nonlinear motion of beam particles, especially at large amplitude, is an essential issue. In this paper, we discuss influences of intrinsic nonlinear fields in the RCS and the combined effect with the space charge, based on single- and multi-particle tracking simulations.

INTRODUCTION

The 3-GeV rapid-cycling synchrotron (RCS) of J-PARC is designed to provide a 1-MW proton beam at a repetition rate of 25 Hz for the injection energy of 400 MeV [1]. The injection energy to the RCS at the first stage is 181 MeV, which is to be finally upgraded to 400 MeV.

The key issue in the design of high intense proton machines is to control and localize the beam loss and to decrease the uncontrolled beam loss. One of the main sources of the beam loss is the space-charge defocusing force. In order to control the beam density and to suppress the space-charge effect, a transverse painting injection is to be performed at the RCS. An adequate ratio between the physical and collimator apertures is another important factor to localize the beam loss. The painting emittance and collimator acceptance are each 216π and 324π mm mrad. In order to gain a sufficient collimation efficiency ($\sim$99.7%), a large ring acceptance of 486π mm mrad is secured for a possible momentum spread of $\pm1\%$.

In this kind of proton synchrotrons with large bore, intrinsic nonlinear magnetic fields play a significant role, and the nonlinear motion of beam particles, especially moving away from the axis of the elements, is an essential issue. The leading source of nonlinear fields at the RCS is the sextupole magnets utilized for the chromatic correction. In addition, there can exist significant nonlinear field components in the fringes of the main dipole and quadrupole magnets because of the large aspect ration of the magnets (inner diameter over magnet length). These nonlinear fields can excite different high-order structure resonances, rending the motion of beam particles at large amplitude and causing a shrinkage of the dynamic aperture. Therefore the working point should be chosen so as to avoid such nonlinear resonances as well as linear resonances. However, even so a portion of the beam particles could cross some of the resonances and be lost, as the space charge of the beam plays a defocusing role, pulling down the betatron tunes of the beam particles, and also the space-charge itself can be the driving term of nonlinear resonances. For these concerns, we have first investigated the nonlinear single-particle dynamics, especially the limitation of the dynamic acceptance, and then the nonlinear effect combined with the space charge by multi-particle tracking simulations. In addition, a possible cure for the induced nonlinear resonances is discussed in this paper.

* hotchi.hideaki@jaea.go.jp

INTRINSIC NONLINEAR FIELDS IN THE J-PARC RCS

The multipole field components of the dipole and quadrupole magnets are listed in Table 1, which were evaluated with their measured and simulated (TOSCA) field distributions corresponding to the lower injection energy of 181 MeV. The multipole field for each magnet was introduced into our tracking simulations as plural thin lenses so as to reproduce the field profile [2]. The natural chromaticity of the RCS is ~-9.0 for both horizontal and vertical, which is to be corrected by three families of sextupole magnets. The sextupole strengths required for the linear chromatic correction are also listed in Table 1.

NONLINEAR SINGLE-PARTICLE DYNAMICS

We performed single-particle tracking simulations with a code called SAD [3], investigating the nonlinear behavior of the single particle at the injection energy of 181 MeV. As listed in Table 1, the chromatic correction sextupole magnets were excited, and the multipole field components of the dipole and quadrupole magnets were included up to 14-pole. In this simulation, the synchrotron oscillation was included assuming the stationary bucket. The physical apertures were set for all the main magnets and for a beam particle with the initial condition of ϵ_x=ϵ_y, x=$\sqrt{\epsilon_x/\gamma_x}$, x'=0, y=$\sqrt{\epsilon_y/\gamma_y}$, y'=0, z=0, $\delta p/p$=0 or 0.5% we looked for the maximum value of ϵ_x=ϵ_y for which the beam survived within the physical apertures up to 5000 turns, where (x,x'), (y,y') and (z, $\delta p/p$) are the transverse and longitudinal phase space coordinates, ϵ is the emittance and γ=(1+α^2)/β of the betatron amplitude functions. As shown in Fig. 1-(a) and (b), several nonlinear structure resonances coming from the three-fold symmetric lattice of the RCS appear in the nominal operating region. The strong sextupole fields required for the chro-

Table 1: Strengths of nonlinear field components ($K_n = \frac{1}{B\rho}\int \frac{\partial^n B_y}{\partial x^n} ds$) of each magnet evaluated for the working tune of (6,72,6.35); multipole field components of the dipole and quadrupole magnets at the injection energy of 181 MeV, and sextupole fields required for the chromatic correction sextupole magnets.

Magnet type	Family name (number)	K_0	K_1 (m^{-1})	K_2 (m^{-2})	K_3 (m^{-3})	K_4 (m^{-4})	K_5 (m^{-5})	K_6 (m^{-6})
Dipole	BM (24)	2.618E-1	-2.023E-2	-1.006E-1	3.635E-1	-1.332E+1	2.340E+2	-6.370E+4
Quadrupole	QFL (6)	-	1.937E-1	-	7.545E-2	-	1.966E+1	-
Quadrupole	QDL (6)	-	-2.054E-1	-	-8.000E-2	-	-2.084E+1	-
Quadrupole	QFM (3)	-	2.016E-1	-	5.677E-2	-	1.168E+2	-
Quadrupole	QFN (12)	-	2.321E-1	-	1.906E-1	-	3.686E+2	-
Quadrupole	QDN (12)	-	-2.320E-1	-	-1.905E-1	-	-3.685E+2	-
Quadrupole	QFX (12)	-	1.593E-1	-	7.947E-2	-	1.547E+2	-
Quadrupole	QDX (9)	-	-2.125E-1	-	-1.745E-1	-	-3.376E+2	-
Sextupole	SDA (6)	-	-	-3.169E-1	-	-	-	-
Sextupole	SDB (6)	-	-	-2.671E-1	-	-	-	-
Sextupole	SFX (6)	-	-	4.170E-1	-	-	-	-

matic correction strongly excite the $Q_x - 2Q_y$=−6 resonance. In addition, different higher-order resonances, such as $2Q_x - 2Q_y$=0, $Q_x - 4Q_y$=−18, etc., are induced directly by the higher-order nonlinear field components or / and by the strong sextupole component through the 2^{nd}-order perturbation expansion. The $4Q_x$=27 can also strongly be excited by the sextupole and octupole components, while their contributions to the driving term are just compensated with each other in this condition.

Correction of the 3^{rd}-order structure resonance

The 3^{rd}-order $Q_x - 2Q_y$=−6 resonance makes the strongest limitation for the dynamic acceptance. Therefore the working tune should be chosen below the resonance in this case, otherwise a part of the beam particles could get at the resonance and be lost, due to the space-charge tune depression. Thus, in order to gain better stability and flexibility of the betatron phase space, the correction of the $Q_x - 2Q_y$=−6 is essential. For this concern, we have discussed additionally introducing two families of sextupole correctors at both ends of the dispersion-free insertion. The driving term of the $Q_x - 2Q_y$=−6 resonance is expressed as $G_{1,-2,-6}e^{j\zeta} = -\frac{\sqrt{2}}{8\pi}\oint[\frac{B_y^{(2)}}{B\rho}\sqrt{\beta_x\beta_y^2} \times exp\ j\{\chi_x(s) - 2\chi_y(s) - (Q_x - 2Q_y + 6)\theta\}]ds$, where χ is the phase advance and θ the orbiting angle. The real and imaginary parts of the driving term for the sextupole field component of the dipole and chromatic correction magnets, which were estimated to be 0.906+j0.182 at the resonant tune of (6.68, 6.34), can be compensated by the resonance correctors with moderate sextupole field strengths of ∼0.1 m^{-2}. As shown in Fig. 1-(c) and (d), the $Q_x - 2Q_y$=−6 resonance significantly declines in the nominal operating region for both on- and off-momentum particles through this resonance correction.

SPACE-CHARGE SIMULATIONS

In order to observe the combined effect of the intrinsic nonlinear fields and space charge, and to verify

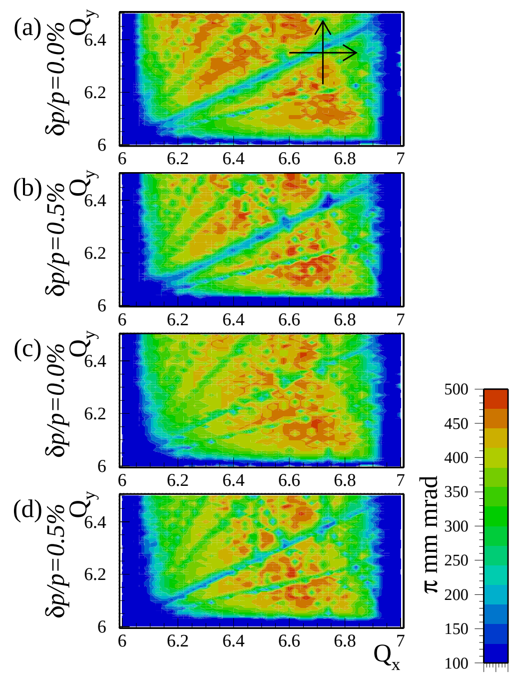

Figure 1: Dynamic acceptance maps as a function of Q_x and Q_y estimated for on- and off-momentum particles of $\delta p/p$=0 and 0.5% in the nominal operating region. The upper (a) and (b) show those before the correction of $Q_x - 2Q_y$=−6, while the lower (c) and (d) are after that.

the effectiveness of the 3^{rd}-order resonance correction, space-charge simulations were performed with a fully 3D particle-in-cell code called SIMPSONS [4]. In the simulations, 2×10^5 macro-particles, a transverse grid of 50 $(r)\times64$ (θ) in the polar coordinate for the radius of the conducting boundary of 0.17 m and a longitudinal grid of 100 (z) were employed, and all the physical quantities and operating parameters were chosen according to the specifications in the design. The injection energy and output beam power assumed are 181 MeV and 0.6 MW. In terms of the space-charge effect, this situation is severe rather than that for the 1-MW output with the 400-MeV injection energy at the final goal. The simulations were implemented for the injection and early stage of the acceleration period up

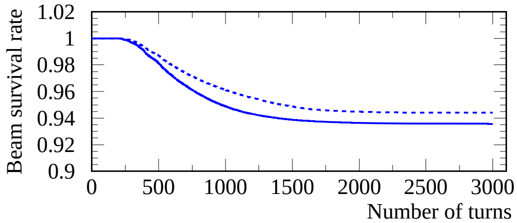

Figure 2: Beam survival as a function of turn number estimated for the bare working tune of (6.72, 6.35) without any resonance correction, in which the solid line shows the result from a simulation including all the intrinsic nonlinear fields listed in Table 1, while the dotted line is that including only the chromatic correction sextupole fields.

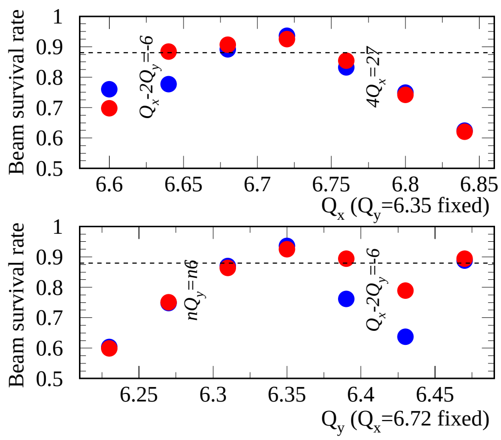

Figure 3: Beam survival rate at 3000 turns as a function of the working tune along the scanning lines shown in Fig 1-(a), in which the blue and red circles correspond to those without and with the $Q_x - 2Q_y$=-6 resonance correction, and the dotted line shows the threshold corresponding to the limit of beam losses at the collimator (4 kW).

to 3000 turns corresponding to ∼550 MeV, with the chromatic correction. As for the multipole field components of the dipole and quadrupole magnets, their strengths estimated at the injection energy were scaled by the momentum rigidity according to the acceleration.

Fig. 2 shows the beam survival as a function of turn number without any resonance correction. In the simulations, the bare working point was set at (6.72, 6.35), which is just below the structure resonances of $Q_x - 2Q_y$=-6 and $4Q_x$=27. The solid line in the figure shows the result from a simulation including all the intrinsic nonlinear fields listed in Table 1, while the dotted line is that including only the chromatic correction sextupole fields. As most of the beam particles are far from the 3^{rd}- and 4^{th}-order resonances in this period thanks to the incoherent tune shift of∼0.35, 1% difference of the beam losses stands for the influence of higher-order resonances such as $Q_x - 4Q_y$=-18.

Fig. 3 plots the beam survival rate at 3000 turns for different working points along the scanning lines shown in Fig. 1-(a), in which the blue and red circles correspond to those without and with the 3^{rd}-order resonance correction, and the dotted line shows the threshold corresponding to the limit of beam losses at the collimator (4 kW). In the figure, there are degradations of the beam survival corresponding to the effects of $Q_x - 2Q_y$=-6 and $4Q_x$=27. The $Q_x - 2Q_y$=-6 resonance is strongly excited mainly by the chromatic correction sextupole fields, while the $4Q_x$=27 resonance, to which the contributions of the sextupole and octupole fields are small as mentioned in the last section, is driven mainly by the space-charge force. In addition, the beam loss increases in the lower region of the vertical tune. This is caused by several structure resonances of nQ_y=$n6$ piling up on the Q_y=6 line, where n is integer. By the correction of the $Q_x - 2Q_y$=-6 resonance mentioned in the last section, the corresponding beam loss is recovered. In the simulations, the sextupole field strengths of the resonance correctors were fixed for all the operating tunes. Therefore, this situation should be still improved by optimizing them according to the choice of the operating tune. Anyway the present simulations recommend the operation around (6.72, 6.35) at which the nonlinear effects can be minimized in this case. In addition, as for the 0.6 MW operation in the lower injection energy of 181 MeV involving the strong space-charge effect, the 3^{rd}-order resonance correction will be useful to get a margin for the large incoherent tune shift and also to get alternate working points such as the interspace of the $nQ_x - nQ_y$=0 and $Q_x - 2Q_y$=-6 resonances.

SUMMARY

For the J-PARC RCS, we investigated influences of the intrinsic nonlinear fields, and the combined effect with the space charge, based on single- and multi-particle tracking simulations including the multipole field components of the dipole and quadrupole magnets, and the chromatic correction sextupole fields. Several nonlinear structure resonances were observed in the nominal working region, in which the $Q_x - 2Q_y$=-6 mainly driven by the chromatic correction sextupole fields and $4Q_x$=27 induced through the space charge can lead to significant beam losses and strongly limit the tunability of the RCS. As for the $Q_x - 2Q_y$=-6 resonance, the driving term can be compensated with two families of sextupole correctors with moderate field strengths. By the resonance correction, it was shown the corresponding beam loss is recovered. This resonance correction should be effective for high intense operations involving a large incoherent tune shift, such as the 0.6 MW operation in the lower injection energy of 181 MeV.

REFERENCES

[1] “Accelerator Technical Design Report for High-Intensity Proton Accelerator Facility Project”, JAERI-Tech 2003-044.

[2] H. Hotchi *et al.*, “Evaluation of nonlinear effects in the 3-GeV Rapid Cycling Synchrotron of J-PARC”, Proc. of 2005 Particle Accelerator Conference, p.916, 2005.

[3] http://acc-physics.kek.jp/SAD/sad.html.

[4] S. Machida and M. Ikegami, “Simulation of Space Charge Effects in a Synchrotron”, AIP Conf. Proc. 448, p.73, 1998.